

Intrinsic Thermal Vibrations of Suspended Doubly Clamped Single-Wall Carbon Nanotubes

B. Babić, J. Furer, S. Sahoo, Sh. Farhangfar, and C. Schönenberger*

Institut für Physik, Universität Basel, Klingelbergstr. 82, CH-4056 Basel, Switzerland

Received July 3, 2003; Revised Manuscript Received September 1, 2003

ABSTRACT

We report the observation of thermally driven mechanical vibrations of suspended doubly clamped carbon nanotubes, grown by chemical vapor deposition (CVD). Several experimental procedures are used to suspend carbon nanotubes. The vibration is observed as a blurring in images taken with a scanning electron microscope. The measured vibration amplitudes are compared with a model based on linear continuum mechanics.

Carbon nanotubes (NTs) form a material with unique mechanical properties.^{1–5} The high Young's modulus and low specific weight qualify single-wall carbon nanotubes (SWNTs) as ultimate mechanical resonators. Similar to lithographically patterned SiC beams, whose resonance frequency has recently crossed the border from MHz to GHz,⁶ it would be highly desirable to integrate NTs into nanoelectromechanical systems (NEMSs) and to electrically excite the mechanical vibration modes.⁷ A first step in this direction has been the observation of electrically driven mechanical vibrations of multiwall carbon nanotubes.³ Nanometer-sized resonators oscillate at high frequencies, but simultaneously have small vibration amplitudes, which are difficult to measure. At cryogenic temperatures, the resonant adsorption of an external electromagnetic field could successfully be measured using superconducting elements attached to a freely suspended NT.⁸ At room temperature a tunneling probe in the form of, for example, an STM tip would be a versatile detector. Integrating a sensitive measuring transducer with a NT nanomechanical oscillator is, however, challenging. In a first step, it would be desirable if the mechanical vibrations could be imaged directly. Here, we report on the observation of thermal vibrations of suspended doubly clamped SWNTs, imaged by scanning electron microscopy (SEM).

Thermally driven excitations of multiwall carbon nanotubes (MWNTs), clamped at one end only, were first investigated by Treacy et al.¹ The mechanical oscillation appeared in the images, which were collected with a transmission electron microscope (TEM), as a blurring that increased toward the free end of the MWNTs.

To see whether a similar experiment is possible with doubly clamped SWNTs, we will first estimate the expected amplitude in thermal equilibrium at room temperature. A

schematic diagram with coordinate system is shown in Figure 1a. Assuming that linear continuum mechanics is a good approximation, the equation of motion for the vertical displacement ξ is given by⁹

$$\frac{\partial^2 \xi}{\partial t^2} + \left(\frac{YI}{\rho A} \right) \frac{\partial^4 \xi}{\partial x^4} = 0 \quad (1)$$

Here, ρ is the mass density, A the cross-sectional area, Y the Young's modulus, and $I = \pi d^4/64$ the moment of inertia, which depends only on the diameter d . Applying the boundary conditions for doubly clamped beams, i.e., $\xi = 0$ and $\xi' = 0$ at the two boundaries, the spectrum of eigenfrequencies is obtained:

$$\omega_i = \frac{\beta_i^2}{L^2} \sqrt{\frac{YI}{\pi d \rho_{2d}}} \quad (i = 1, 2, 3, \dots) \quad (2)$$

where L is the suspended length, ρ_{2d} is the surface mass density of a graphite sheet (7.7×10^{-7} kg m⁻²) and $\beta_1 = 4.73$, $\beta_2 = 7.85$, and $\beta_3 = 11.0$ for the first three modes.

The equipartition theorem predicts that each vibration mode carries the energy $k_B T$ in thermal equilibrium at temperature T , where k_B is the Boltzmann constant. Together with the appropriate solutions of eq 1, one obtains an expression for the variance of the maximum deflection amplitude, which for the fundamental frequency ($i = 1$) occurs in the middle:

$$\sigma_1^2 \equiv \langle \xi_1^2(L/2) \rangle = \frac{k_B T L^3}{\gamma_1 Y I} \quad (3)$$

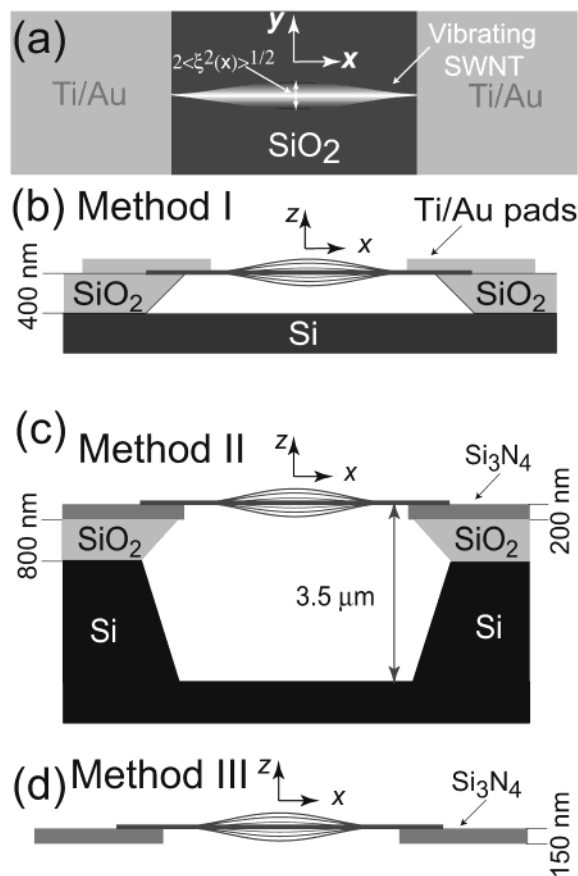


Figure 1. Schematic drawings of doubly clamped vibrating SWNT which are suspended by different methods. (a) top view, (b–d) side views.

Table 1. Characteristic Quantities of Suspended SWNT ($d = 1.5$ nm, $Y = 1$ TPa)^a

L (μm)	ω (MHz)	σ_1 (nm)
0.2	4600	0.8
0.5	740	3.4
1	185	9.3
3	21	48.3
5	7.4	104

^a The eigenfrequencies and maximum thermal amplitudes are calculated using relations (2) and (3), respectively.

where $\gamma_1 = 192$.¹⁰ Table 1 summarizes the eigenfrequencies and the thermal vibration amplitudes at room temperature of a “typical” SWNT with diameter $d = 1.5$ nm and Young’s modulus $Y = 1$ TPa for different (practically feasible) suspension lengths $L = 0.2$ – 5 μm . This table demonstrates that thermal vibration amplitudes can be of appreciable magnitude, of order ≈ 10 nm ($L = 1$ μm). Since state-of-the-art scanning electron microscopes have resolutions well below 10 nm, thermal vibration should appear on SEM images.

There are already many reports on the fabrication of suspended NTs. For example, SWNTs were grown between distant silicon towers,^{11,12} spread over metal posts,¹³ or grown over solid terraces¹⁴ and etched trenches.⁴ Though devices with suspension lengths of $L \gtrsim 5$ μm were realized and imaged with SEM, the thermal vibration has surprisingly not

yet been reported, although it should readily have shown up in respective SEM images, provided the reported SWNTs were *single* SWNTs. In the work of Dai and co-workers,^{11,12,14} the SWNTs were coated with a metal layer to increase the contrast in the SEM, whereas others have explicitly reported on suspended *ropes* of SWNTs or MWNT,^{5,13} which are inherently stiffer.

Carbon nanotubes are synthesized by chemical vapor deposition (CVD) as previously reported.¹⁵ We would like to emphasize that not all grown NTs are individual SWNTs. This will be explained further in the text. To account for the possible influence of substrate during imaging in SEM, we have suspended NTs using three different methods.

Method I, shown in Figure 1b, is based on the work of Nygård et al.¹⁶ The NTs are grown on thermally oxidized (400 nm) Si substrates. Electrical contacts are patterned by electron-beam lithography (EBL), followed by evaporation (Ti/Au) and lift-off. The SiO₂ is etched in buffered HF.¹⁷ To stop etching, the sample is heavily rinsed in water followed by 2-propanol. With this method we find it possible to suspend NTs over distances up to 1 μm . For larger lengths, the surface tension of the etchant tends to pull the NT down to the substrate.

In method II, shown in Figure 1c, the NTs are grown across predefined trenches. We start with a Si substrate with layers of 800 nm of SiO₂ and 200 nm of Si₃N₄. Slits of width 1–5 μm and length 10 μm are first etched into the top Si₃N₄ layer using a CHF₃-based plasma etching process.¹⁹ Next, the slit is further wet-etched into SiO₂ and the Si substrate using HF and KOH,²⁰ respectively. This results in deep trenches ~ 3.5 μm , a prerequisite for NTs to bridge the trenches in the CVD growth process.

In method III, shown in Figure 1d, slits are defined in Si₃N₄ membranes of thickness 150 nm and lateral size 0.5 mm following a procedure similar to that in method II.

The key difference between the three methods is the depth of suspension. It is 400 nm, 3.5 μm , and ∞ for methods I–III, respectively. The samples are imaged with SEM (Philips XL30 FEG) at room temperature. To generate an image, a focused electron beam is raster scanned.

To deduce the vibration amplitude quantitatively, two assumptions have to be made: (1) the intensity profile of the electron beam centered at coordinate (x, y) has a Gaussian distribution and (2) the measured intensity of secondary electrons reflects the (time-averaged) probability $P(x, y) \equiv P_x(\xi)$ to find the NT at position (x, y) convoluted with the intensity profile of the primary beam. (1) is a convenient assumption and (2) should hold, because scanning in SEM is slow as compared to the vibration of the NT. The latter results in a blurring of the NT in SEM images. An example of a vibrating suspended NT is shown in Figure 2a. The vibration is observed as a blurring, which is largest in the middle. In contrast, the NT appears sharp at the edges of the trench, limited by the finite resolution of the SEM. To deduce the vibration amplitude, more precisely the variance $\sigma^2(x) \equiv \langle \xi^2(x) \rangle$, we note that $P_x(\xi)$ is Gaussian and determined by Boltzmann statistics. The deconvolution is simple because of assumption (1). We only need to extract $\sigma^2(x)$ from the

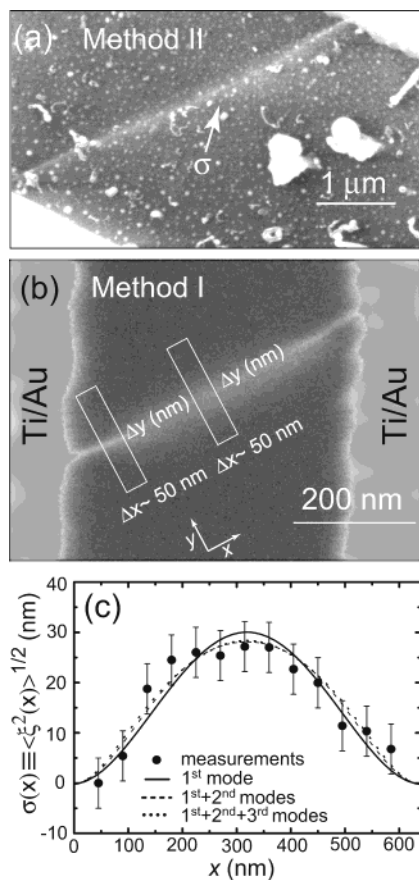


Figure 2. (a) SEM image of a vibrating SWNT grown over a trench. A strong blurring is clearly visible (indicated by arrows), which is a consequence of intrinsic thermal vibrations. (b) Another vibrating NT, whose root-mean-square displacement along x is plotted in (c). Circles are measured points and the curves represent fits.

intensity distribution of the SEM image perpendicular to the NT and subtract $\sigma^2(0)$. To do so, we average the intensity profile in Δx slices as shown in Figure 2b and fit it to a Gaussian. Such an analysis was first done for MWNT cantilevers by Krishnan et al.¹⁸

Figure 2b shows a SEM image of a suspended doubly clamped vibrating NT fabricated by method I. The free suspension length is relatively short, i.e., $L \approx 650$ nm. Applying the analysis procedure mentioned above, the maximum rms vibration amplitude is determined to be $\sigma = 27 \pm 5$ nm. We have also analyzed σ as a function of x and compare the result with analytical curves for the first three eigenmodes in Figure 2c. The agreement between the measured points and the theoretical curves is reasonably good. Matching between experiment and theory is improved if the first *and* second modes are taken into account, each of which carries kT energy. Contributions from higher order modes decay very rapidly and can be neglected. Note, there is one fitting parameter Yd^4 , which will be discussed below.

Figure 3a shows another NT grown over a Si_3N_4 membrane. Here, the suspension length is rather large, i.e., $L \approx 6.2$ μm . Correspondingly, the observed blurring is much larger. The maximum rms vibration amounts to $\sigma = 80 \pm 5$ nm. Applying eq 3 and assuming the typical high Young's

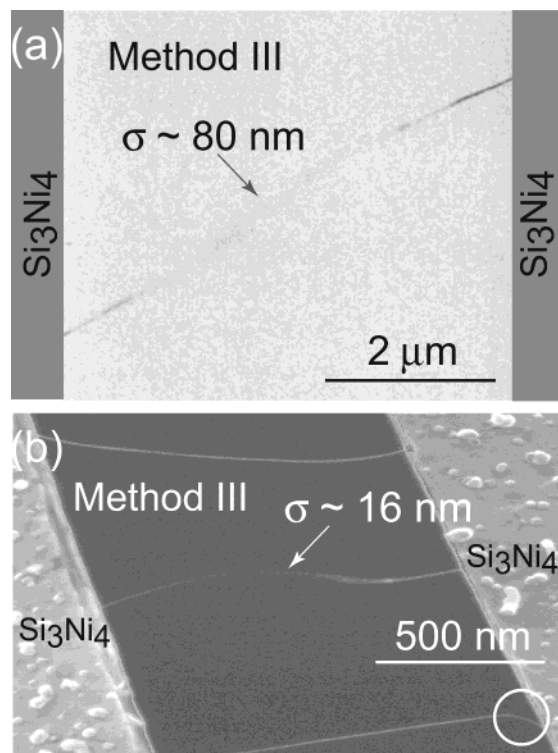


Figure 3. (a) SEM image of long ($L \approx 6.2$ μm) vibrating SWNT grown over a slit in a Si_3N_4 membrane. In (b), three NTs are imaged simultaneously. Only the middle one is vibrating. A white circle indicates branching of the lower NT into two NTs.

modulus value of SWNTs of $Y = 1$ TPa, the diameter of this NT is estimated to be $d = 2 \pm 0.5$ nm.

The SEM image displayed in Figure 3b shows three suspended NTs. Though grown in one run, only one NT seems to vibrate, namely the middle one. This, at first sight surprising result, points to a variability of NTs that are grown during one and the same process. The only parameter in our experiment that is not predetermined is Yd^4 , see eq 3. Though different values for the Young's modulus were reported, we suspect that the diameter d is the cause for the variability, because it enters in the fourth power. The absence of visible vibrations for the upper and lower NT in Figure 3b suggests that these have a larger diameter. They may be multiwall nanotubes or ropes of tubes. In fact, the lower one must be a rope, because a clear branching is observed at the right end (highlighted by a circle). Having looked through a large number of samples, the fraction of vibrating tubes is very small (a few %). This is a clear indication that not all of the grown NTs are SWNTs.

We summarize the measured rms vibration of several NTs in Table 2. Determined are L and $\sigma(L/2)$. Using eq 3, we obtain an estimate for Yd^4 , which is given in the third column. What is immediately noticed is the large spread in Yd^4 of more than 2 orders of magnitude. Unfortunately, we are not able to unambiguously deduce the Young's modulus Y and diameter d , independently. We have tried to measure the diameter using atomic force microscopy (AFM). Due to surface roughness and the strong d^4 dependence, the error bar is too large to deduce Y with an acceptable accuracy. For the discussion we instead rely on an average diameter

Table 2. Properties of Some Vibrating NTs^a

L (μm)	σ (nm)	Yd^4 (GPa (nm) ⁴)	$Y_{1.6}$ (GPa)	d_1 (nm)	method
0.55	25	117	18	0.58	I
0.63	27	150	23	0.62	I
1.35	16	4221	644	1.4	III
4.05	85	4038	616	1.4	II
4.30	90	4311	658	1.45	II
6.25	80	16754	2556	2.0	III

^a L is the suspended length, σ the measured maximum rms vibration, Yd^4 obtained using eq 3, $Y_{1.6}$ Young's modulus assuming $d = 1.6$ nm (see text), and d_1 the NT diameter assuming $Y = 1$ TPa.

for SWNTs, which we have obtained from electrical measurements of contacted semiconducting NTs.¹⁵ We have analyzed the band-gap, which is inversely proportional to the diameter d , of more than 10 semiconducting SWNTs and obtained as an average $d = 1.6 \pm 0.3$ nm. We note that, taking this diameter, the estimated Young's modulus (column 4 in Table 2, denoted by $Y_{1.6}$) has an accuracy of "only" 75%. Well graphitized NTs have a large Young's modulus. For example, $Y = 1.4 \pm 0.4$ TPa was reported for SWNTs grown by laser ablation,¹⁸ whereas 1 TPa was found in simulations independent of helicity and number of shells.²¹ In column 5 of Table 2 we therefore also list the diameter d_1 , which we deduce from the measured Yd^4 , assuming $Y = 1$ TPa; d_1 varies between 0.58 and 2.0 nm. Since we have never observed SWNTs with diameters < 1 nm in TEM, the first two NTs (row 1 and 2), both belonging to samples prepared by method I, cannot have a large Young's modulus $Y \sim 1$ TPa. Taking d to be 1.6 nm leads to a modulus of only $Y_{1.6} \approx 20$ GPa. Because method I uses HF-etching, it is possible that the NT's are affected during this process step. It is also possible that the under-etching changes the clamping conditions (boundary conditions) at the edges. In contrast to method I, the as-grown CVD NTs of methods II and III yield consistent results, which are in agreement with a large Young's modulus of 1 TPa and with the diameter, which we have deduced by electrical measurements. Though we observe ropes and small diameter MWNTs (only a few number of shells) in TEM, their diameter is typically larger than 2 nm. This strongly suggests that the NTs of row 3–6 in Table 2 are *single-wall* carbon nanotubes.

To our knowledge there are no reports on the Young's modulus of CVD-grown SWNTs. Though we are not able to accurately determine Y , our results suggest that CVD-grown SWNTs can have a large modulus of order $Y \approx 1$ TPa. The exception are wet-etched NTs, for which our data suggest $Y \ll 1$ TPa. Small Young's modulus have previously been reported for CVD-grown MWNTs.²²

In conclusion, we have demonstrated that it is possible to observe thermally driven vibrations of suspended doubly

clamped SWNTs in SEM. From the measured rms vibration amplitude, the Young's modulus Y of CVD-grown SWNTs has been estimated. Only a small fraction of suspended NTs are seen to vibrate, although they are suspended over a comparable length and grown at the same time. This suggests that the majority of grown tubes are *not* single SWNTs, but rather ropes and MWNTs, a finding, which is supported by TEM. We suspect that this is the reason why thermal vibrations of SWNTs has not already been observed before.

Acknowledgment. We acknowledge support and technical assistance with TEM imaging by A. Engel, G. Gantenbein, and H. Stahlberg of the Biocenter and discussions with L. Forró. This work has been supported by COST (BBW), the Swiss NFS, and the NCCR on Nanoscience. This section tagged TF_References_Section

References

- (1) Treacy, M. M. J.; Ebbesen, T. W.; Gibson, J. M. *Nature* **1996**, *381*, 678.
- (2) Lourie, O.; Wagner, H. D. *J. Mater. Res.* **1998**, *13*(9), 2418.
- (3) Poncharal, P.; Wang, Z. L.; Ugarte D.; Heer, W. A. *Science* **1999**, *283*, 1513.
- (4) Walters, D. A.; Ericson, L. M.; Casavant, M. J.; Liu J.; Colbert, D. T.; Smith, K. A. Smalley, R. E. *Appl. Phys. Lett.* **1999**, *74*, 3803.
- (5) Yu, M. F.; Lourie, O.; Dyer, M. J.; Moloni, K.; Kelly T. F.; Ruoff, R. S. *Science* **2000**, *287*, 637.
- (6) Ming, X.; Huang, H.; Zorman, C. A.; Mehregany, M.; Roukes, M. L. *Nature* **2003**, *421*, 496.
- (7) Roukes, M. L. *Phys. World* **2001**, *14*, 25.
- (8) Reulet, B.; Kasumov, A. Yu.; Kociak, M.; Deblock, R.; Khodos, I. I.; Gorbatov, Yu. B.; Volkov, V. T.; Journet, C.; Bouchiat H. *Phys. Rev. Lett.* **2000**, *85*, 2829.
- (9) See, e.g., Landau L. D.; Lifschitz E. M. *Theory of Elasticity*; Pergamon Press: New York, 1959.
- (10) Sapmaz, S.; Blanter, Ya. M.; Gurevich L.; van der Zant, H. S. J. *Phys. Rev. B* **2003**, *67*, 235414.
- (11) Cassell, A. M.; Franklin, N. R.; Tomblor, T. W.; Chan, E. M.; Han, J.; Dai, H. *J. Am. Chem. Soc.* **1999**, *121*, 7975.
- (12) Franklin, N. R.; Dai, H. *Adv. Mater.* **2000**, *12*, 890.
- (13) Kim, G.; Gu, G.; Waizmann, U.; Roth, S. *Appl. Phys. Lett.* **2002**, *80*, 1815.
- (14) Franklin, N. R.; Wang, Q.; Tomblor, T. W.; Javey, A.; Shim, M.; Dai, H. *Appl. Phys. Lett.* **2002**, *81*, 913.
- (15) Babić, B.; Iqbal, M.; Schönenberger, C. *Nanotechnology* **2003**, *14*, 327.
- (16) Nygård, J.; Cobden, D. H. *Appl. Phys. Lett.* **2001**, *79*, 4216.
- (17) Buffered hydrofluoric acid is made according to the following recipe: 28 mL HF + 107 mL H₂O + 113 g NH₄F. The etch rate for SiO₂ is 50 nm/min.
- (18) Krishnan, A.; Dujardin, E.; Ebbesen, T. W.; Yianilos, P. N.; Treacy, M. M. J. *Phys. Rev. B* **1998**, *58*, 14013.
- (19) Tilman Hoss, Ph.D. Thesis, University of Basel, pp 22, 2000.
- (20) The etch ratio of Si to SiO₂ is ≈ 500 , for 20% weight mass of KOH at 60 °C.
- (21) Lu, J. P. *Phys. Rev. Lett.* **1997**, *79*, 1297.
- (22) Salvétat, J.-P.; Kulik, A. J.; Bonard, J.-M.; Andrew, G.; Briggs, D.; Stöckli, T.; Méténier, K.; Bonnamy, S.; Béguin, F.; Burnham, N. A.; Forró, L. *Adv. Mater.* **1999**, *11*, 161.

NL0344716